Eurasian Chem.-Technol. J. 27 (2025) 101–110
The journal of the Institute of Combustion Problems https://ect-journal.kz

https://doi.org/10.18321/ectj1658

Modification of Diatomite Mineral Sorbent for the Cleanup of Petroleum Spills on Water Surfaces

Nur-Sultan Mussa[1], Kanat Amantaiuly[2], Seitkhan Azat[3], Rachid Amrousse[4], Kainaubek Toshtay[2]*

[1]Université de Lille, F-59000 Lille, France
[2]Al-Farabi Kazakh National University, 71 al-Farabi ave., Almaty, Kazakhstan
[3]Satbayev University, 22a Satpaev str., Almaty, Kazakhstan
[4]Chouaïb Doukkali University, Faculty of Sciences, El Jadida, Morocco

Article info

Received:
14 March 2025

Received in revised form:
10 April 2025

Accepted:
25 May 2025

Keywords:
Diatomite
Oil spills
Sorbent
Sorption capacity
Acid treatment

Abstract

The study investigates the structural, thermal, and adsorption properties of natural diatomite and its modified forms (thermally and acid-treated) for oil spill remediation. X-ray diffraction analysis revealed amorphous silica alongside crystalline phases. Thermogravimetric analysis showed mass losses at 80–300 °C (removal of adsorbed water) and 430–700 °C (dehydroxylation), with an 8.63% total mass loss. Acid treatment with 0.5N H_2SO_4 significantly altered the chemical composition, increasing the SiO_2 content to 88.8% while dissolving CaO, Na_2O, and MnO_2. Infrared spectroscopy confirmed the removal of hydroxyl groups and structural changes following treatment. Nitrogen adsorption analysis revealed enhanced porosity in the acid-modified diatomite (D-H_2SO_4-400), showing a BET surface area of 80.0 m^2/g and a uniform pore size distribution of 19.0 nm. Scanning electron microscopy revealed preserved skeletal structures with improved porosity. Oil sorption tests showed that D-H_2SO_4-400 exhibited the highest adsorption capacity (optimal at 4 g, 30 µm particle size), achieving maximum uptake within 2 minutes. Overall, these findings confirm that thermal and acid treatments enhance the sorption efficiency of diatomite, making it a promising low-cost and environmentally friendly material for oil spill remediation.

1. Introduction

Accidental spills of petroleum products pose a serious threat to the environment. These incidents may occur during oil extraction, processing, or transportation. In recent years, their ecological consequences have become increasingly evident, with oil spills significantly disrupting ecosystems and damaging habitats [1]. The long-term environmental impact remains difficult to predict, as oil contamination interferes with natural processes and alters the living conditions for a wide range of organisms [2]. Addressing such spills requires a comprehensive response strategy that combines various technical methods and resources. Regardless of the type of petroleum product involved, the immediate priority is localized containment to prevent further spread and reduce the extent of environmental damage [3].

The removal of petroleum product spills involves several methods: thermal, mechanical, biological, and physicochemical [4]. Mechanical oil recovery is one of the primary methods for eliminating oil and petroleum product spills. It is most effective in the first few hours after a spill, as the oil layer remains relatively thick at this stage. This is crucial, as factors like a thin oil layer, widespread distribution, and the constant movement of the surface layer due to currents and wind hinder the process of separating oil from water. Additionally, complications may arise when cleaning oil and petroleum product contamination in port areas and shipyards. These areas are

*Corresponding author.
E-mail address: kainaubek.toshtay@kaznu.kz

often polluted with debris-such as boards, splinters, and other floating objects – that complicate the cleanup process [5].

The thermal method of oil spill remediation is based on the ignition of the oil layer. This method can be applied when the oil layer is thick enough and immediately after the spill, before emulsions with water have formed [6].

The biological method of oil spill remediation is applied after the mechanical and physicochemical methods have been used, when the oil film thickness is greater than 0.1 mm [7]. The physicochemical method involving the use of sorbents and dispersants is effective when mechanical collection of oil and petroleum products is not possible, such as when the oil film is too thin or when oil spills present a real threat to the most ecologically sensitive areas [8, 9].

Every year, humanity spends millions of dollars on the aftermath of oil and petroleum product spills. Therefore, the technology for oil and petroleum spill remediation is particularly relevant today. Naturally, such a technology must meet modern requirements – it should be as accessible and convenient as possible, environmentally friendly, and economically feasible [10, 11].

We have conducted a search and analysis of patent and scientific-technical literature on the remediation of emergency oil spills [12–15]. The analysis of methods and techniques for localizing and remediating oil and petroleum product spills suggests that the most effective solution to the problem is the use of sorbents – substances that absorb or adsorb oil. Currently, there are approximately two hundred different sorbents known worldwide, used in oil spill remediation. These sorbents are classified according to their composition into inorganic, natural and synthetic organic, and biological categories [16]. During the extraction, transportation, and processing of oil, significant quantities of oil and petroleum products are spilled due to various accidents. As a result, the land becomes saturated with oil, or an oil film forms on the surface of the sea [17]. Between 1970 and 2018, during the transportation of oil by sea, an average of 5.87 million tons of oil was spilled into the sea due to accidental tanker accidents and damage [18].

Such extensive marine pollution causes irreversible damage to the ecosystem, disrupting the physical, chemical, and biological balances in the environment. Therefore, the remediation of oil and petroleum product spills is one of the most urgent and important tasks.

The objective of this study is to develop an environmentally sustainable and efficient technology for treating oil-contaminated water using a sorbent derived from domestic diatomite. Owing to its highly porous structure, diatomite is utilized across various industries: as an oil sorbent in environmental applications [19], a filtration agent in the food and pharmaceutical sectors [20], a fungicidal material in agriculture [21], a catalyst support in chemical processes [22, 23], and an insulating material in construction [24]. By leveraging the unique properties of diatomite a natural, abundant, and eco-friendly mineral this research aims to develop a cost-effective solution that minimizes environmental impact while effectively removing oil and petroleum-based contaminants from aquatic environments. The proposed technology holds promise as a safer and more sustainable alternative to conventional oil spill remediation methods. This study introduces a novel approach using locally sourced diatomite as a sustainable, cost-effective sorbent for oil spill remediation. Unlike previous works, it focuses on optimizing domestic diatomite's properties for aquatic environments, providing an eco-friendly alternative to conventional and imported sorbents through enhanced performance and accessibility.

2. Experimental

2.1 Method for preparing the sorbent

Natural diatomite from the Aktobe deposit (Kazakhstan) was selected as a sorbent for oil removal from water surfaces. To achieve the desired physicochemical properties, the material underwent chemical and thermal treatment. The preparation process included drying, fractionation, and impurity removal. Sulfuric acid was used as a modifying agent, with optimized treatment conditions involving specific temperature, duration, filtration, and washing to a neutral pH. The modified samples were further ground and fractionated by particle size [25].

Experimental batches of diatomite processed under various conditions were obtained to investigate its chemical composition and physicomechanical properties. As a sorbent material, natural diatomite (D) was first thermally treated at 400 °C (D-400) for 4 h, then mixed with sulfuric acid (0.5N H_2SO_4: diatomite = 1:3). The mixture was heated at 90-100 °C with continuous stirring for 3 h (300 RPM), followed by filtration, washing to neutral pH, and fine grinding (D-400-H_2SO_4) [26].

2.2 Physicochemical characteristics of the diatomite

Thermogravimetric analysis (TGA) was performed using an STA 449C Jupiter instrument (NETZSCH, Germany) over a temperature range of 40–1000 °C under ambient air conditions. The heating rate was set at 5 °C per minute. The microstructure of the samples was examined using scanning electron microscopy (SEM) with a Hitachi SU8010 electron microscope at an accelerating voltage of 5 kV. Infrared (IR) spectra of the samples were recorded using a Perkin Elmer Spectrum 65 spectrometer in the range of 400–4000 cm^{-1} with a scanning resolution of 4 cm^{-1}. The spectra were obtained from pressed KBr pellets prepared at a ratio of 1 mg of sample to 200 mg of KBr. The elemental composition of diatomite was analyzed using X-ray fluorescence (XRF) spectroscopy with a sequential spectrometer Axios Max (PANalytical, Netherlands). The maximum tube voltage was 25 kV, and the maximum anode current was 144 mA. Textural properties of the synthesized samples were determined based on nitrogen adsorption-desorption isotherms at 77 K, obtained using a volumetric analyzer ASAP 2020 (Micromeritics, USA). The specific surface area was calculated using the Brunauer-Emmett-Teller (BET) method, while the average pore diameter was estimated by the Barrett-Joyner-Halenda (BJH) method from the desorption branch of the isotherm. Prior to the measurements, the samples were degassed at 200 °C under a residual pressure of 10^{-3} mmHg for 4 hours. X-ray diffraction analysis (XRD) was carried out using a D8 Advance powder X-ray diffractometer (Bruker) with CuKα radiation (λ = 0.15406 nm). The measurement conditions were: scanning step size – 0.1°, counting time – 2 sec per point, tube voltage and current – 40 kV and 40 mA, respectively. The scanning range was 2θ = 4–80°.

2.3 The oil sorption tests

To absorb the crude oil layer, 200 ml of artificial tap water was poured into a 250 ml beaker. Then, crude oil was added to form a layer of a specified thickness. After that, the sorbent was spread over the surface of the oil layer. After a certain absorption time, the sorbent was removed using a net. These tests were carried out in a static system without stirring. All sorption experiments were performed in triplicate, and the sorption capacity of the sorbent was calculated using the following equation.

$$\text{Oil sorption capacity} = \frac{\text{weight of sorbent (g)}}{\text{weight of adsorbed oil (g)}}$$

3. Results and Discussion

3.1 Characterization of the diatomite

The XRD pattern of natural diatomite is shown in Fig. 1. The pattern of the untreated diatomite sample (D) exhibits a broad halo, indicating the presence of amorphous silica. Superimposed on this diffuse background are several distinct diffraction peaks corresponding to crystalline phases. The peak at 2θ = 21.57° is characteristic of cristobalite, while the reflection at 2θ = 23.46° corresponds to α-tridymite. A prominent peak at 2θ = 26.56° is attributed to α-quartz. Additionally, the reflection at 2θ = 29.31° (d = 3.041 Å) indicates the presence of calcite in the sample.

Thermogravimetric analyses were conducted to assess the physical-mechanical properties and thermal stability of the initial diatomite sample. The analysis results are shown in Fig. 2.

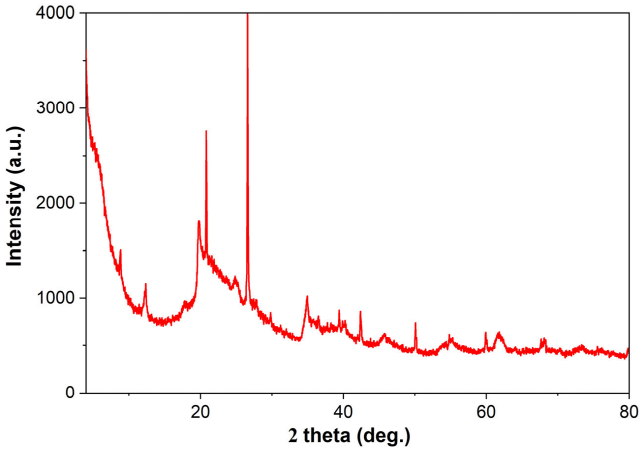

Fig. 1. X-ray diffraction pattern of the initial diatomite.

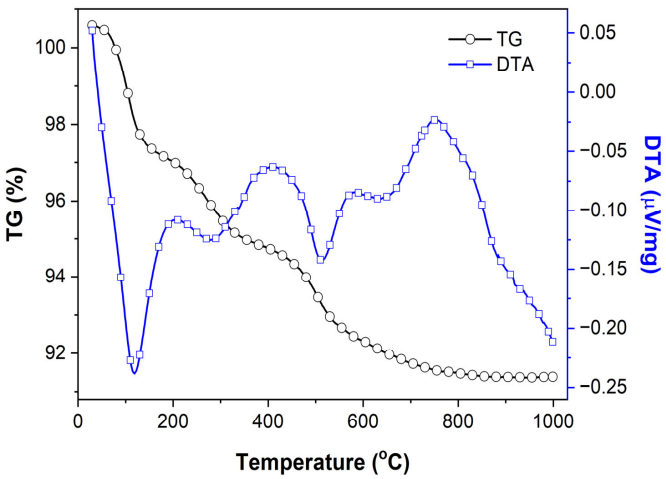

Fig. 2. Thermal (TG-DTA) curves of the initial diatomite.

As shown in Fig. 2, the mass of the sample primarily decreases in the temperature ranges of 80–300 °C and 430–700 °C. The DSC curve of this sample exhibits three endothermic peaks at 119 °C, 250 °C, and 515 °C. The endothermic peaks at 119 °C and 250 °C are attributed to the removal of surface and physically adsorbed water from the diatomite. The endothermic effect at 515 °C is explained by the removal of chemically bound water or the elimination of hydroxyl groups from the structure of kaolinite and montmorillonite [27]. As the temperature increases, a distinct exothermic effect is observed on the thermogram, with a minimum at 750 °C, which is attributed to the crystallization of diatomite particles. The total mass loss of the sample, determined from the TG curve in the temperature range of 20–1000 °C, is 8.63%.

Prior to their use as adsorbents, clay mineral ores such as diatomite, montmorillonite, and bentonite typically undergo thermal and chemical treatments to increase their specific surface area, modify pore structure, and enhance adsorption capacity [28, 29]. In this study, the elemental composition of natural, thermally treated, and acid-treated diatomite samples was analyzed using X-ray fluorescence spectrometry. Based on the elemental analysis, the chemical composition of each sample was calculated, and the average oxide content is summarized in Table 1.

As seen in Table 1, the results of the X-ray fluorescence analysis show that the main components of the natural diatomite are SiO_2 (74.52%) and Al_2O_3 (13.85%). Upon treatment of the diatomite with 0.5 N H_2SO_4, along with a reduction in the mass fractions of K_2O, Fe_2O_3, MgO, and Al_2O_3, certain oxides (CaO, Na_2O, and MnO_2) completely dissolve from the diatomite.

Figure 3 shows the IR spectra of diatomite samples (D, D-400, D- H_2SO_4-500) in the frequency range of 400–4000 cm^{-1}.

As shown in Fig. 3, the IR spectra of all diatomite samples exhibit strong absorption bands at 1031 and 1103 cm^{-1}, which correspond to the valence vibrations of the Si-O-Si bond. We can also observe weaker absorption bands for Si-O-Si bonds in tetrahedral coordination (799 cm^{-1}) and bands associated with the valence deformation vibrations of OH groups (3441 and 1632 cm^{-1}) from physically adsorbed water molecules. Notably, these IR spectra are in good agreement with the data presented in works [30, 31].

From Fig. 3b, after thermal and acid treatment of the initial diatomite (Fig. 4a), peaks corresponding to the absorption bands of SiOH, Al-Al-OH (915 cm^{-1}), and OH groups associated with kaolinite (3621 and 3694 cm^{-1}) disappear, indicating a dehydration process. During acid activation of the diatomite, the intensity of the Si-O-Al absorption band (536 cm^{-1})

Table 1. Comparison of the chemical composition of treated diatomite samples with the original

Diatomite samples	Oxide content, mass %								
	SiO_2	Al_2O_3	Fe_2O_3	TiO_2	Na_2O	CaO	K_2O	MgO	MnO_2
D	74.52	13.85	4.54	0.90	1.34	0.44	1.48	0.83	0.08
D-400	77.12	11.82	4.16	0.90	1.24	0.31	1.42	0.78	0.06
D-400-H_2SO_4	88.79	8.92	0.52	0.90	0.00	0.00	0.65	0.32	0.00

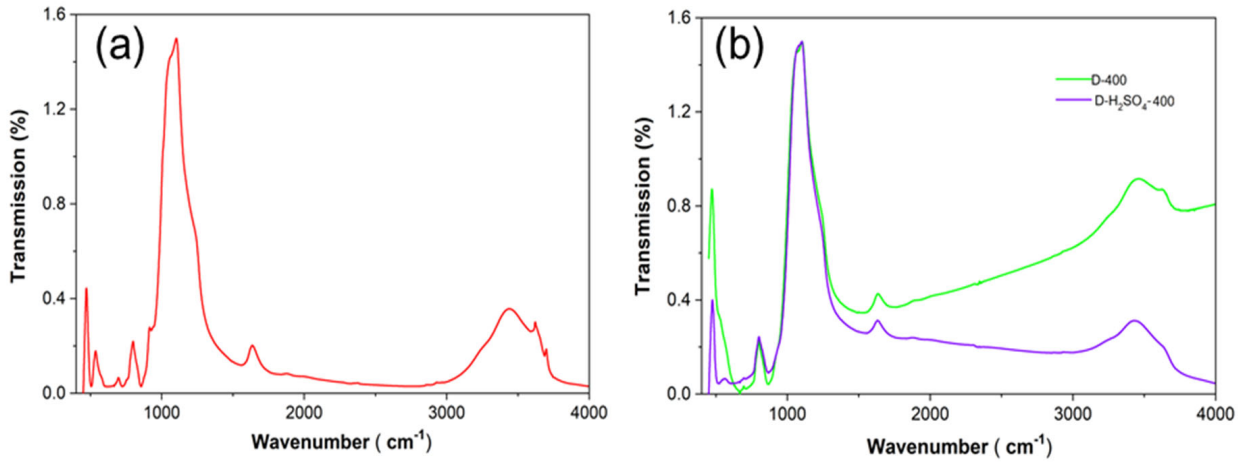

Fig. 3. IR spectra of diatomite samples: (a) raw diatomite and (b) thermal and acid treated diatomite.

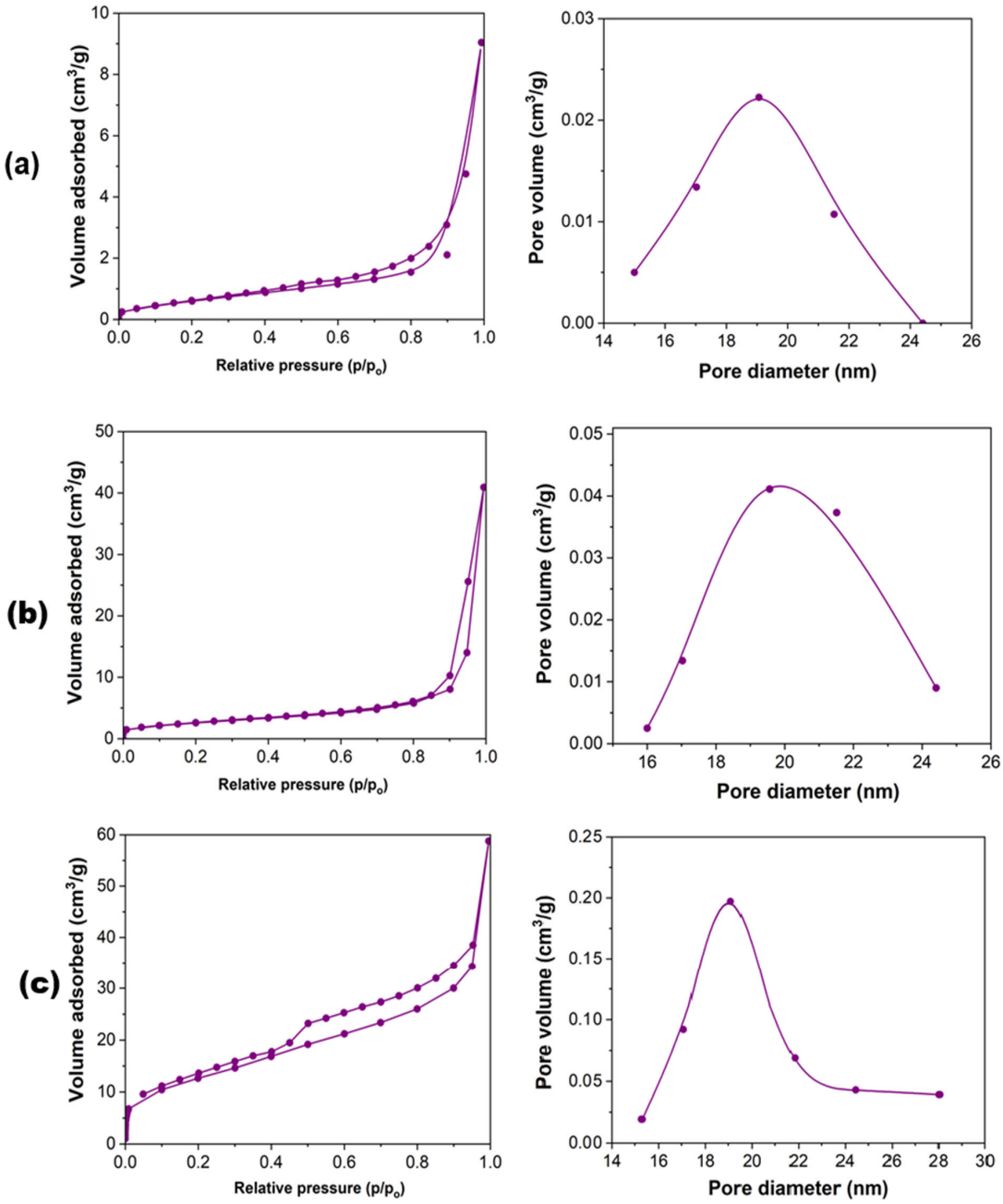

Fig. 4. Adsorption isotherms and pore size distribution of diatomite samples: (a) D, (b) D-400 and (c) D- H_2SO_4-400.

decreases due to the removal of the hexacoordinated aluminum cation from the octahedral layer [32]. When diatomite is modified with acids, Ca^{2+} and Mg^{2+} ions in the crystal lattice are replaced by hydrogen ions, resulting in the formation of the H-form of the adsorbent. While the original structure of the crystal lattice is preserved, the nature and porosity of the surface undergo significant changes [33].

Figure 4a and 4b illustrate the adsorption isotherms for diatomite samples (D, D-400, D-HCl-500) and the corresponding differential pore size distribution curves obtained using the BJH method.

The nitrogen adsorption isotherms of the original and thermally treated diatomite exhibit minimal gas uptake (Fig. 4a), indicating weak adsorption. However, in the relative pressure region, the isotherm of the acid-modified diatomite (D-H_2SO_4-400) displays a sharp increase in adsorption. The corresponding isotherm curve for D-H_2SO_4-500 features a pronounced hysteresis loop, suggesting enhanced porosity and a more uniform pore size distribution.

BET surface area analysis showed that the specific surface areas of the raw diatomite (D), thermally treated (D-400), and acid-modified (D-H_2SO_4-400) diatomite samples were 10.0, 17.0, and 80.0 m^2/g, respectively. Furthermore, BJH pore size distribution analysis revealed an average pore diameter of 19.0 nm (Fig. 4b).

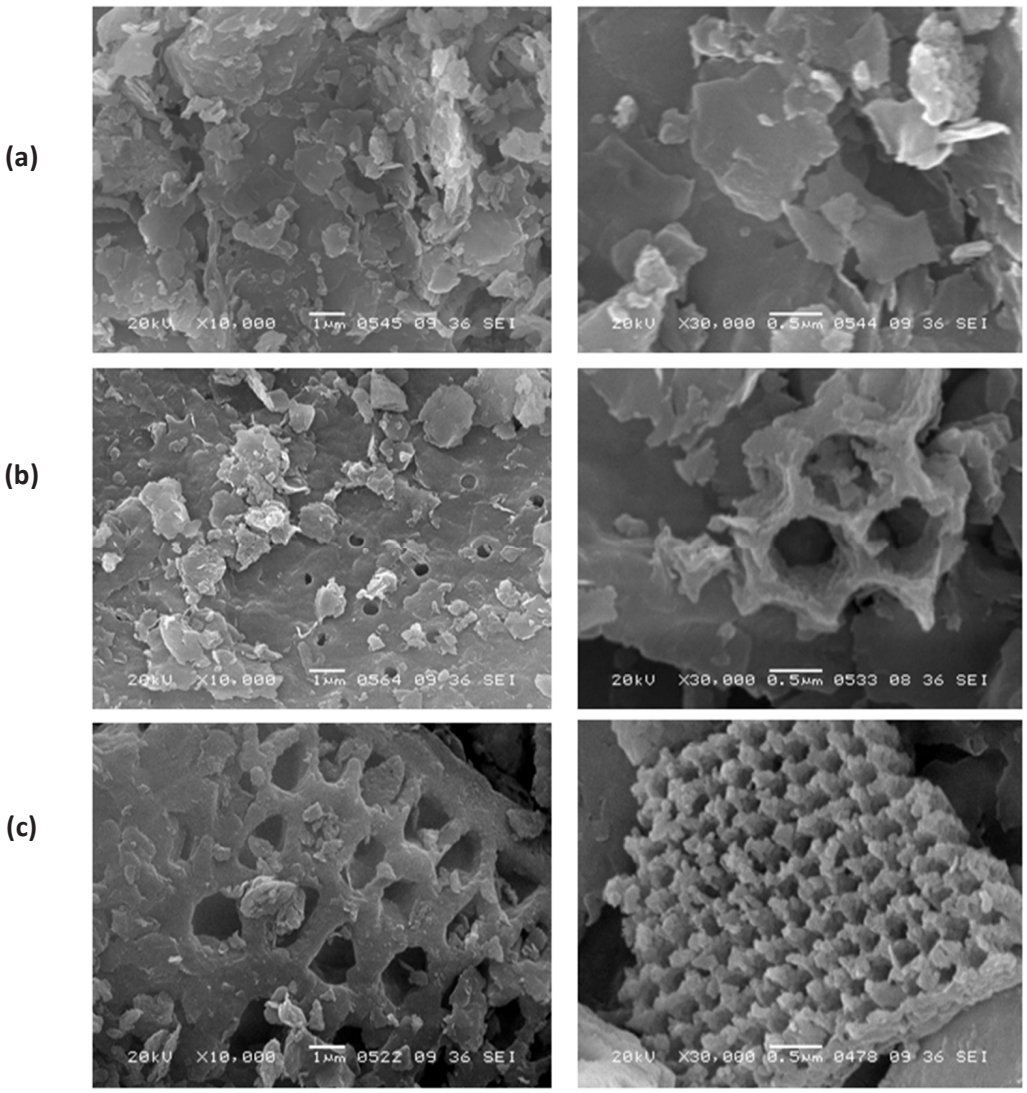

Fig. 5. SEM images of the diatomite samples: (a) D, (b) D-400 and (c) D-H_2SO_4-400.

The SEM images (Fig. 5a, b, c) show that there are observable differences in the surface structures of the raw and modified diatomite samples; however, the original skeleton and crystalline lattice structure are preserved. Notably, the samples depicted in Fig. 5a and 5b exhibit a well-developed porous structure, indicating the successful formation of porosity during the modification process.

3.2 Oil sorption tests

The dependence of sorption capacity on (a) different types of diatomite, (b) the mass of activated diatomite, (c) particle size of activated diatomite, and (d) contact time is presented in Fig. 6. As shown in Fig. 6a, the acid-activated diatomite sample (D-H_2SO_4-400) demonstrated the highest sorption capacity for crude oil from the Kumkol oil field. This enhanced performance can be attributed to the combined effects of thermal treatment and acid activation, which significantly influence the morphological structure and surface properties of the diatomite. Figure 6b indicates that a diatomite mass of 4 g yielded the maximum oil sorption capacity. Although the same oil mass was used in all experiments, the increased adsorption capacity with 4 g of adsorbent (Fig. 6b) is attributed to enhanced oil retention resulting from better surface interaction and saturation efficiency at this dosage. These findings highlight the importance of optimizing sorbent characteristics and conditions to achieve maximum efficiency. In Fig. 6c, the sorption efficiency of various particle size fractions (all at 4 g) was assessed using the optimized diatomite dosage. The results show that particles with an average size of 30 μm exhibited the highest sorption capacity. Moreover, as illustrated in Fig. 6d, the maximum oil uptake was achieved within just 2 min of contact time, indicating the rapid sorption kinetics of the activated diatomite.

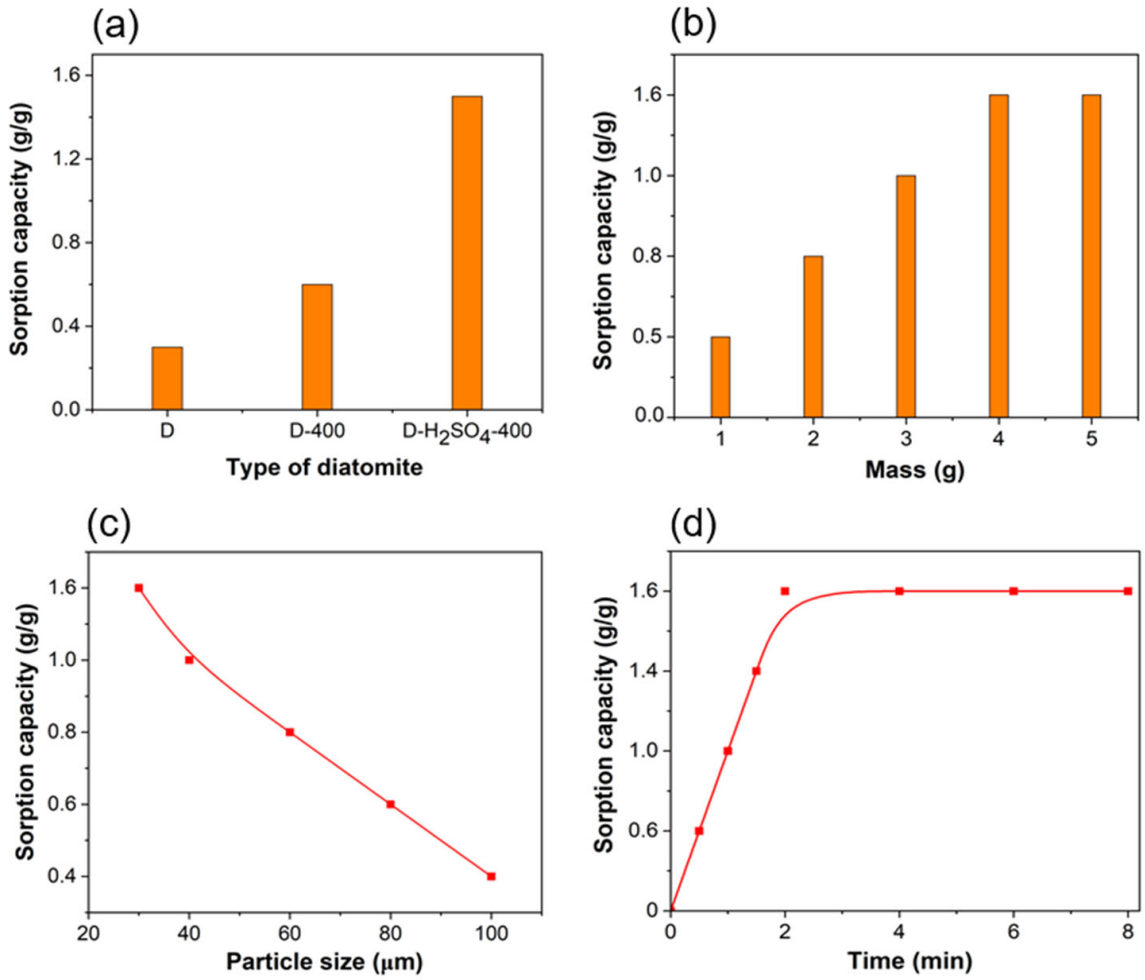

Fig. 6. Dependence of sorption capacity on (a) different types of diatomite, (b) the mass of activated diatomite, (c) particle size of activated diatomite, and (d) contact time.

After each adsorption cycle, the modified diatomite was mechanically squeezed to recover the absorbed oil. For the next 6 cycles, the sorbent was washed with toluene after mechanical squeezing. The washing process involved three rinses with toluene to ensure the complete removal of residual oil from the sorbent. After washing, the sorbent was again squeezed to remove excess solvent and then dried at 90–100 °C for 50 minutes. The dried sorbent was subsequently reused for the next adsorption cycle. Figure 7 presents the reusability performance of the modified diatomite in sorption applications. The oil recovery performance of modified diatomite decreased gradually over seven consecutive adsorption cycles. Initially, the sorbent recovered approximately 1.6 g of oil per gram of sorbent, corresponding to 100% efficiency. However, with each regeneration cycle – including mechanical squeezing, toluene washing, and drying – the recovery capacity diminished. By the seventh cycle, the recovered oil dropped to around 1.12 g, indicating a 30% decline in efficiency. This reduction may be attributed to partial pore blockage, structural degradation of the diatomite, or incomplete solvent removal. Despite this decline, the sorbent retained a relatively high level of reusability, demonstrating its potential for multiple-cycle applications in oil spill remediation or recovery processes.

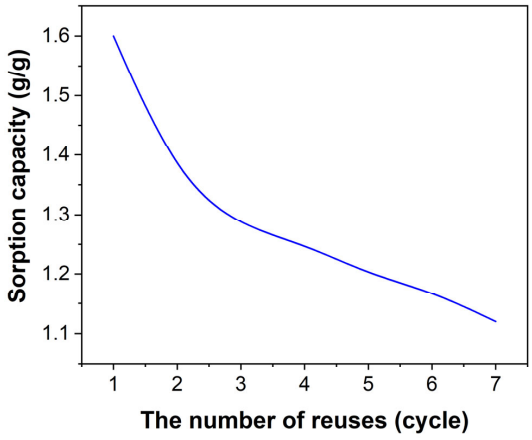

Fig. 7. Evaluation of the reusability of modified diatomite sorbents.

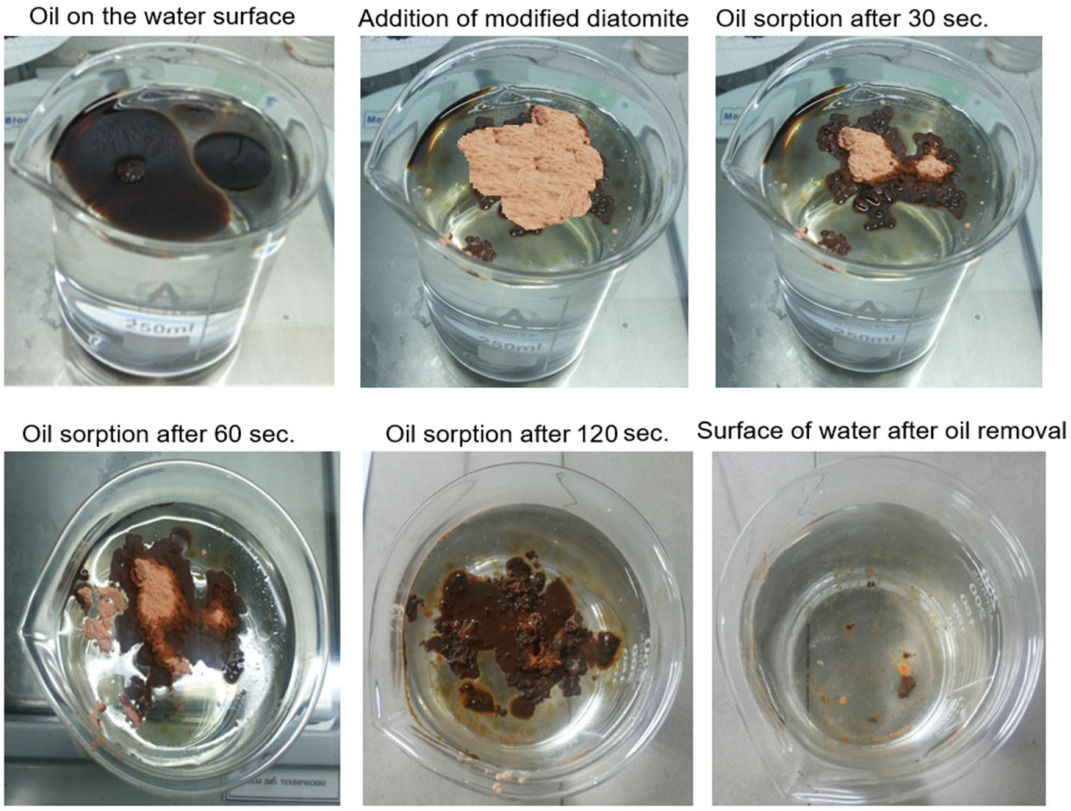

Fig. 8. Sorption of spilled oil from the water surface using activated diatomite (D-H_2SO_4-400).

Figure 8 illustrates the adsorption process of oil from the water surface using modified diatomite. Notably, the sorbent demonstrates rapid adsorption, reaching maximum oil uptake within 2 min, and exhibits excellent buoyancy, which enhances its performance in aquatic environments.

Thermal and acid treatments significantly alter the elemental composition of diatomite. Specifically, modification with 0.5 N sulfuric acid leads to an increase in SiO_2 content, accompanied by a reduction in Al_2O_3, Fe_2O_3, Na_2O, CaO, and MgO levels. The results indicate that acid treatment enhances the oil sorption capacity of the studied natural mineral materials, with the extent of improvement varying depending on the type and concentration of the acid used.

4. Conclusions

This study demonstrated that thermal and acid modifications significantly enhance the structural and sorption properties of natural diatomite. Acid treatment with 0.5 N H_2SO_4 notably increased the SiO_2 content while reducing the concentration of impurities, resulting in greater surface area and improved porosity. Among the samples, the acid-modified diatomite (D-H_2 SO_4-400) exhibited the highest oil sorption capacity, particularly for 30 µm oil droplets, achieving maximum adsorption within just 2 minutes. In addition to its rapid sorption kinetics, the material maintained excellent buoyancy, making it highly effective for cleaning oil spills from water surfaces. These findings underscore the potential of modified diatomite as a low-cost, efficient, and environmentally sustainable sorbent for petroleum spill remediation.

Acknowledgements

This study was supported by the Science Committee of the Ministry of Science and Higher Education of the Republic of Kazakhstan (AP23489574).

References

[1]. H. Bi, Z. Wang, R. Yue, et al., Oil spills in coastal regions of the Arctic and Subarctic: Environmental impacts, response tactics, and preparedness, *Sci. Total Environ.* 958 (2025) 178025. DOI: 10.1016/j.scitotenv.2024.178025

[2]. B. Zhang, E.J. Matchinski, B. Chen, et al., Marine oil spills-oil pollution, sources and effects (Chapter 21)., World Seas: An Environmental Evaluation (Second Edition) Volume III: Ecological Issues and

Environmental Impacts (2019) 391–406. DOI: 10.1016/B978-0-12-805052-1.00024-3

[3]. G. Cumo, F., Gugliermetti, G. Guidi, Best available techniques for oil spill containment and clean-up in the Mediterranean Sea, *WIT Trans. Ecol. Environ.* 103 (2007). DOI: 10.2495/WRM070491

[4]. I.C. Ossai, A. Ahmed, A. Hassan, F.S. Hamid, Remediation of soil and water contaminated with petroleum hydrocarbon: A review, *Environ. Technol. Innov.* 17 (2020) 100526. DOI: 10.1016/j.eti.2019.100526

[5]. B. Liu, B. Chen, J. Ling, et al., Development of advanced oil/water separation technologies to enhance the effectiveness of mechanical oil recovery operations at sea: Potential and challenges, *J. Hazard. Mater.* 437 (2022) 129340. DOI: 10.1016/j.jhazmat.2022.129340

[6]. Si-Zhong Yang, Hui-Jun Jin, Zhi Wei, et al., Bioremediation of oil spills in cold environments: a review, *Pedosphere* 19 (2009) 371–381. DOI: 10.1016/S1002-0160(09)60128-4

[7]. M. Baniasadi, S.M. Mousavi, (2018). A Comprehensive Review on the Bioremediation of Oil Spills. In: Kumar, V., Kumar, M., Prasad, R. (eds) Microbial Action on Hydrocarbons. Springer, Singapore. DOI: 10.1007/978-981-13-1840-5_10

[8]. S. ben Hammouda, Z. Chen, C. An, K. Lee, Recent advances in developing cellulosic sorbent materials for oil spill cleanup: A state-of-the-art review, *J. Clean. Prod.* 311 (2021) 127630. DOI: 10.1016/j.jclepro.2021.127630

[9]. A. Dhaka, P. Chattopadhyay, A review on physical remediation techniques for treatment of marine oil spills, *J. Environ. Manage*. 288 (2021) 112428. DOI: 10.1016/j.jenvman.2021.112428

[10]. K. Sharma, G. Shah, H. Singh, et al., Advancements in natural remediation management techniques for oil spills: challenges, innovations, and future directions, *Environmental Pollution and Management* 1 (2024) 128-146. DOI: 10.1016/j.epm.2024.08.003

[11]. J. Cisneros-Aguirre, M. Afonso-Correa, Integrated application of innovative technologies for oil spill remediation in gran tarajal harbor: A scientific approach, *Waste* 2 (2024) 414–450. DOI: 10.3390/waste2040023

[12]. Patent US8388849B2, Publ., (2013) J. M. Sherman. Method and apparatus for skimming oil from water using absorbent pads.

[13]. Patent RU2223920C1, Publ., (2004) V.I. Pavlenko, O.N. Aminov, D.I. Fozekosh, R.N. Jastrebinskij. Method of treating waste waters to remove oil products.

[14]. Patent US20120087730A1. Publ., (2012) N.T. Berger J, Sorbent boom.

[15]. N. Bhardwaj, A.N. Bhaskarwar, A review on sorbent devices for oil-spill control, *Environ. Pollut.* 243 (2018) 1758–1771. DOI: 10.1016/j.envpol.2018.09.141

[16]. A.T. Hoang, X.P. Nguyen, X.Q. Duong, T.T. Huynh, Sorbent-based devices for the removal of spilled oil from water: a review, *Environ. Sci. Pollut. Res.* 28 (2021) 28876–28910. DOI: 10.1007/s11356-021-13775-z

[17]. N.N.C. Samsuria, W.Z.W. Ismail, M.N.W.M. Nazli, et al., Problems, effects, and methods of monitoring and sensing oil pollution in water: A review, *Water* 17 (2025) 1252. DOI: 10.3390/w17091252

[18]. B.L. Chilvers, K.J. Morgan, B.J. White, Sources and reporting of oil spills and impacts on wildlife 1970–2018, *Environ. Sci. Pollut. Res.* 28 (2021) 754–762. DOI: 10.1007/s11356-020-10538-0

[19]. M. Łach, K. Pławecka, J. Marczyk, et al., Use of diatomite from Polish fields in sustainable development as a sorbent for petroleum substances, *J. Clean. Prod.* 389 (2023) 136100. DOI: 10.1016/j.jclepro.2023.136100

[20]. U.T. Uthappa, G. Sriram, V. Brahmkhatri,et al., Xerogel modified diatomaceous earth microparticles for controlled drug release studies, *New J. Chem.* 42 (2018) 11964–11971. DOI: 10.1039/C8NJ01238E

[21]. S. Turganbay, S.B. Aidarova, N.E. Bekturganova, et al., Nanoparticles of sulfur as fungicidal products for agriculture, *Eurasian Chem.-Technol. J.* 14 (2012) 313–319. DOI: 10.18321/ectj128

[22]. K. Toshtay, A. Auyezov, Y. Aubakirov, et al., Palladium–nickel supported and palladated activated diatomite as an efficient catalyst for poly-α-olefins hydrogenation, *Catal. Surv. Asia* 27 (2023) 296–305. DOI: 10.1007/s10563-023-09394-y

[23]. K. Toshtay, Liquid-phase hydrogenation of sunflower oil over platinum and nickel catalysts: Effects on activity and stereoselectivity, *Results Eng.* 21 (2024) 101970. DOI: 10.1016/j.rineng.2024.101970

[24]. J.J. Kipsanai, P.M. Wambua, S.S. Namango, S. Amziane, A review on the incorporation of diatomaceous earth as a geopolymer-based concrete building resource, *Materials* (Basel) 15 (2022) 7130. DOI: 10.3390/ma15207130

[25]. K. Toshtay, A.B. Auyezov, Z.A. Bizhanov, et al., Effect of catalyst preparation on the selective hydrogenation of vegetable oil over low percentage

Pd/diatomite catalysts, *Eurasian Chem.-Technol. J.* 17 (2015) 33–39. DOI: 10.18321/ectj192

[26]. K. Toshtay, A.B. Auezov, Hydrogenation of vegetable oils over a palladium catalyst supported on activated diatomite, *Catal. Ind.* 12 (2020) 7–15. DOI: 10.1134/S2070050420010109

[27]. S. Mendioroz, M.J. Belzunce, J.A. Pajares, Thermogravimetric study of diatomites. *J. Therm. Anal.* 35 (1989) 2097–2104. DOI: 10.1007/BF01911874

[28]. A.K. Panda, B.G. Mishra, D.K. Mishra, R.K. Singh, Effect of sulphuric acid treatment on the physico-chemical characteristics of kaolin clay. *Colloids Surfaces A Physicochem. Eng. Asp.* 363 (2010) 98–104. DOI: 10.1016/j.colsurfa.2010.04.022

[29]. K. Gondek, P. Micek, A. Baran, et al., Modified natural diatomite with various additives and its environmental potential, *Materials* 16.12 (2023) 4494. DOI: 10.3390/ma16124494

[30]. J.X. Lin, S.L. Zhan, M.H. Fang, X.Q. Qian, The adsorption of dyes from aqueous solution using diatomite, *J. Porous Mater.* 14 (2007) 449–455. DOI: 10.1007/s10934-006-9039-5

[31]. B.H. Van der Marel H.W., Atlas of infrared spectroscopy of clay minerals and their admixtures., Elsevier, New York. 12 (1977) 279–280. DOI: 10.1180/claymin.1977.012.3.11

[32]. C. Belver, M.A. Bañares Muñoz, M.A. Vicente, Chemical activation of a kaolinite under acid and alkaline conditions, *Chem. Mater.* 14 (2002) 2033–2043. DOI: 10.1021/cm0111736

[33]. P. Yuan, D.Q. Wu, H.P. He, Z.Y. Lin, The hydroxyl species and acid sites on diatomite surface: a combined IR and Raman study, *Appl. Surf. Sci.* 227 (2004) 30–39. DOI: 10.1016/j.apsusc.2003.10.031